



JOINT INSTITUTE FOR NUCLEAR RESEARCH  
Veksler and Baldin laboratory of High Energy Physics

# FINAL REPORT ON THE START PROGRAMME

Pion femtoscopy in Au+Au collisions at  $\sqrt{s_{NN}} = 3$  GeV  
in the STAR experiment

Supervisor: Dr. Alexey Aparin

Student: Anna Kraeva, Russia  
National Research Nuclear University  
MEPhI

Participation period:  
July 17 – September 10,  
Summer Session 2022

Dubna, 2022

# Contents

<b>1</b>	<b>Introduction</b>	<b>2</b>
<b>2</b>	<b>Correlation femtoscopy in nuclear collisions</b>	<b>2</b>
2.1	Experimental correlation function . . . . .	3
2.2	Coordinate system and parameterization of the correlation function . . . . .	4
<b>3</b>	<b>Experiment STAR and collision Data analysis</b>	<b>5</b>
3.1	Results . . . . .	11
<b>4</b>	<b>Summary</b>	<b>14</b>

# 1 Introduction

To date, there is a method that allows you to directly measure the spatio-temporal extent of the hadron production region and the parameters of hadron-hadron interaction, which is called correlation femtoscopy. For the first time, the method of interferometric measurements was proposed by R. Hanbury-Brown and R. Twiss to measure the angular size of stars and other astronomical objects [1] (HBT-method). This method is based on measuring the correlations of the photon double coincidence count intensity depending on the distance between the detectors. The idea was developed in elementary particle physics in the 60s in the work of G. Goldhaber, S. Goldhaber and W. Lee [2], within which the angular distributions of pion pairs during pp-annihilation were considered; in the same work, an increase in the number of like-charged pions with respect to opposite-charged pions was found at small relative angles of expansion. Correlations of this kind are explained by the quantum-statistical properties of the resulting particles: identical bosons (particles with integer spin) which follow the Bose-Einstein statistics are more likely to be born in a close phase space region, while fermions (particles with fractional spin) are less likely due to the Fermi-Dirac statistics properties.

The works of G. Kopylov and M. Podgoretsky [3, 4] can be considered the beginning of a wide application of interferometry to collisions of relativistic nuclei. In the analyzes presented and subsequent to them, the HBT method has become a precision tool for measuring the spatiotemporal properties of regions of homogeneity during kinetic freeze-out (the phase of the evolution of a nucleus-nucleus collision, when the produced particles cease to interact kinetically) during heavy ion collisions. Subsequently, the method of measuring quantum-statistical correlations was called correlation femtoscopy.

In heavy ion collisions, femtoscopy is an important tool for studying the spatiotemporal parameters of a particle emission source. The fundamental tasks of the research are: the search and study of new forms of baryonic matter that have not been observed before, the search for the reasons for the binding of quarks in nucleons, the search for a critical point on the phase diagram of the state of matter.

This work is devoted to the study of two-particle momentum correlations of identical pions in the STAR experiment at the RHIC accelerator, the study and estimation of the size of the emission region of identical pions by constructing the correlation functions of the latter.

## 2 Correlation femtoscopy in nuclear collisions

In elementary particle physics, the HBT method was applied by Goldhaber, Lee and Pais in 1960 at the Bevatron when they studied the angular correlations of identical pions in  $p\bar{p}$  annihilation. It was observed that at low relative momenta an increase in the number of produced pion pairs occurred, which was explained not only by the finite dimensions of the system, but also by its lifetime.

The task of interferometry is to obtain a certain function from the available experimental data, which characterizes the source of emission of particles in the process of collision of heavy nuclei. The HBT method makes it possible to estimate the source size and particle emission time.

To obtain the correlation function of identical bosons, we introduce the symmetrized wave function of their descent [5], which consists of a set of plane waves:

$$\Psi(\vec{x}_1, \vec{x}_2, \vec{p}_1, \vec{p}_2) = \frac{1}{2} \exp(i\vec{p}_1\vec{x}_1 + i\vec{p}_2\vec{x}_2 + i\vec{p}_1\vec{x}_2 + i\vec{p}_2\vec{x}_1), \quad (1)$$

where  $\vec{x}_1$  and  $\vec{x}_2$  - points of emission of bosons with momenta  $\vec{p}_1$  and  $\vec{p}_2$ .

Let the function  $\rho(\vec{x})$  describe the spatial distribution of boson emission points, then the correlation function will take the form:

$$C(\vec{q}) = \int |\Psi_{12}|^2 \rho(\vec{x}_1) \rho(\vec{x}_2) d^3\vec{x}_1 d^3\vec{x}_2 = 1 + |\rho(\vec{q})|^2, \quad (2)$$

where  $\vec{q} = \vec{p}_1 - \vec{p}_2$  - relative momentum.

The solution of the equation above makes it possible to obtain the spatial characteristics of the particle emission region, but not the temporal ones. It is more informative to use one- and two-particle distributions.

The probability of particle escape from the emission region is characterized by the differential interaction cross section  $\frac{d\sigma}{dp}(p)$ . The probability of two particles being emitted is characterized, respectively, by the quantity  $\frac{d^2\sigma}{dp_1 dp_2}(p_1, p_2)$ .

The two-particle correlation function is constructed as the ratio of the two-particle momentum spectrum to the product of two one-particle momentum spectra [6]:

$$C(\vec{p}_1, \vec{p}_2) = N \frac{P(\vec{p}_1, \vec{p}_2)}{P_1(\vec{p}_1) P_2(\vec{p}_2)}, \quad (3)$$

where  $N$  - normalization factor.

In what follows, the two-particle correlation function can be expressed in terms of the variable  $\vec{q}$ .

The theoretical analysis of this formula establishes a connection between the space-time structure of the particle emission source and the experimentally measured correlation function.

## 2.1 Experimental correlation function

The experimental correlation function represents the ratio of the distribution  $A(\vec{q})$  of the relative momenta of pairs of identical bosons from one event to the analogous reference distribution  $B(\vec{q})$ , where quantum-statistical correlations are suppressed:

$$C(q) = \frac{A(\vec{q})}{B(\vec{q})} \quad (4)$$

In the study of two-particle correlations, the choice of the reference distribution plays an important role. The reference distribution should repeat the experimental distribution

except for the presence of quantum-statistical correlations. One of the methods to suppress them was the event mixing method, in which each particle from a pair of particles belonged to different [7] events. Thus, all effects are recreated except for the Bose-Einstein correlations and the interaction in the final state.

## 2.2 Coordinate system and parameterization of the correlation function

For identical particles, the relative momentum  $q$  contains only three independent components, while the source is described by three spatial and one temporal dimensions. As a result, the relative momentum components are expressed in terms of a certain set of correlation radii, depending on the choice of reference system and parameterization.

The most widely used ‘‘Out-Side-Long’’ parameterization is defined as follows. The coordinate system in the space of relative momentum  $\vec{q} = \vec{p}_1 - \vec{p}_2$  of a pair of particles is chosen so that the longitudinal direction long is parallel to the beam axis, the direction out is parallel to the direction of the total transverse momentum of the pair  $\vec{k}_T = (\vec{p}_{1,T} + \vec{p}_{2,T})/2$ , and the side direction is perpendicular to the long and out (fig. 1).

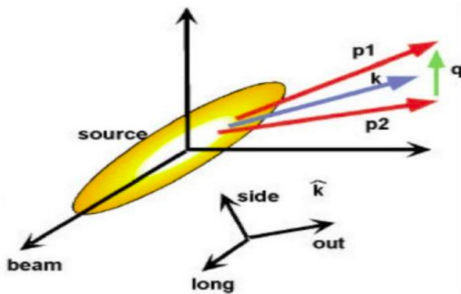


Figure 1: Schematic representation of an LCMS coordinate system

In this paper, we use a longitudinally co-moving coordinate system - Longitudinally Co-Moving System (LCMS) [8], in which  $p_{1z} + p_{2z} = 0$ , where  $p_{1z}$  and  $p_{2z}$  - projections of momenta of the first and second particles onto the  $z$  axis.

The radii of the particle emission region depend on the average transverse momentum of pairs of particles  $k_T$ . In the LCMS system, the correlation function can be represented as the Bowler-Sinyukov function [9]:

$$C(q) = N[(1 - \lambda) + \lambda K(q)(1 + G(q))], \quad (5)$$

where  $\lambda$  is the coefficient characterizing the strength of femtosopic correlations,  $K(q)$  is the Coulomb correction describing the Coulomb repulsion in the case of identical particles,  $N$  is the normalization factor. The function  $G(q)$  - the Gaussian source function - is described by the following equation:

$$G(q) = \exp(-q_o^2 R_o^2 - q_s^2 R_s^2 - q_l^2 R_l^2 - 2q_o q_s R_{os}^2 - 2q_s q_l R_{sl}^2 - 2q_o q_l R_{ol}^2), \quad (6)$$

where  $R_{ij}$  are the corresponding emitter radii (out, side and long).

Experimental correlation functions are usually fitted using the functions 5, 6. The radii extracted after fitting determine not the size of the entire source, but the size of the "homogeneity region" [10], which is a part of the source region emitting particles (fig. 2).

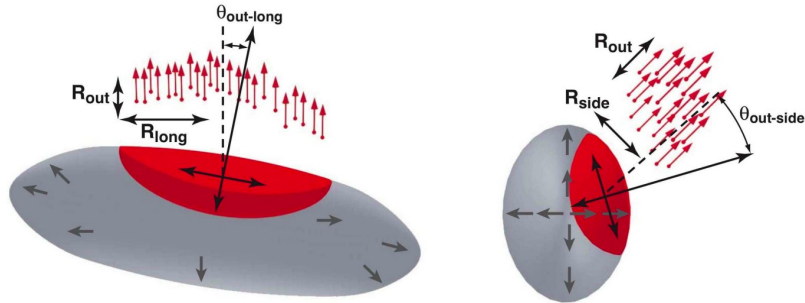


Figure 2: Region of homogeneity of particle emission source. Left - view along the collision axis, right - across the collision axis

The concept of the region of homogeneity was introduced to explain the effect of the dependence of the correlation radii on the transverse momentum of pairs of particles  $k_T$ .

### 3 Experiment STAR and collision Data analysis

The data used for the analysis were obtained in the STAR experiment at RHIC [11]. The minimum bias Au+Au collisions sample at  $\sqrt{s_{NN}} = 3$  GeV were analyzed. The beam was incident on a gold target 0.25 mm thick corresponding to a 1% interaction probability. The target is installed in a vacuum pipe at 200.7 cm west of the STAR center and 2 cm below the beam axis [12].

Each launch of the accelerator is assigned a unique Run Number, which is an eight-digit number YYDDRRR, where 2000+YY-1 is the year, DDD is the day of the year, RRR is the run number on that day. Based on the dependence of the average measured characteristics of collision events, it is possible to exclude RunNumbers that have significant deviations from the general trend. Such numbers may indicate incorrect operation of the detector.

In this analysis, the following RunNumber should be excluded:

19151029, 19151045, 19152001, 19152078, 19153023, 19153032,  
 19153065, 19154012, 19154013, 19154014, 19154015, 19154016,  
 19154017, 19154018, 19154019, 19154020, 19154021, 19154022,  
 19154023, 19154024, 19154026, 19154046, 19154051, 19154056

One of the characteristics of nuclear collisions is multiplicity, which is defined as the number of produced secondary particles per interaction. For a fixed target, particle multiplicity is shown in fig. 3.

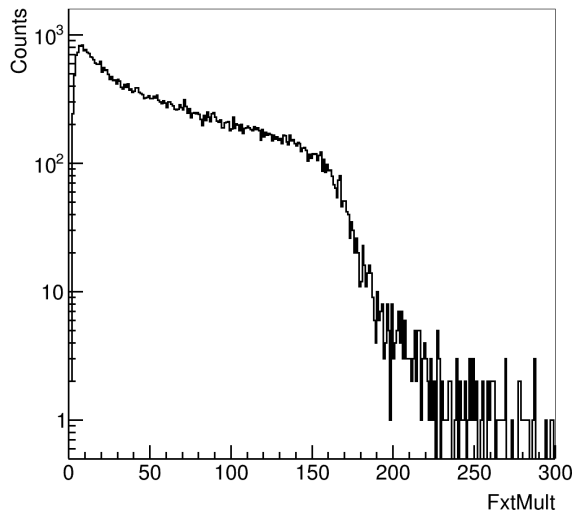


Figure 3: Secondary particle multiplicity distribution

The values of the obtained multiplicity are compared with the ranges of centralities that characterize the degree of overlap of nuclei during a collision. For example, centrality 0% corresponds to central (frontal) collisions, and 100% - to peripheral collisions, where there are no areas of intersection of nuclei. The table 1 shows the correspondence between centralities and multiplicities.

Table 1: Values of Centralities and Multiplicities of Secondary Particles

Centrality	0-5 %	5-10 %	10-15 %	15-20 %	20-25 %	25-30 %
Multiplicity	195-142	141-119	118-101	100-86	85-72	71-60
Centrality	30-35 %	35-40 %	40-45 %	45-50 %	50-55 %	55-60 %
Multiplicity	59-50	49-41	40-33	32-36	25-21	20-16
Centrality	60-65 %	65-70 %	70-75 %	75-80 %		
Multiplicity	15-12	11-9	8-7	6-5		

For the selection of events, the number of which is about  $2.8 \cdot 10^8$  in the data set, the distributions shown in fig. 4 were constructed and the following restrictions were defined:

- $195 < V_z < 205$  cm - the vertex of the collision in the Z axis,
- $V_r < 2$  cm - vertex of collision of nuclei in X and Y coordinates.

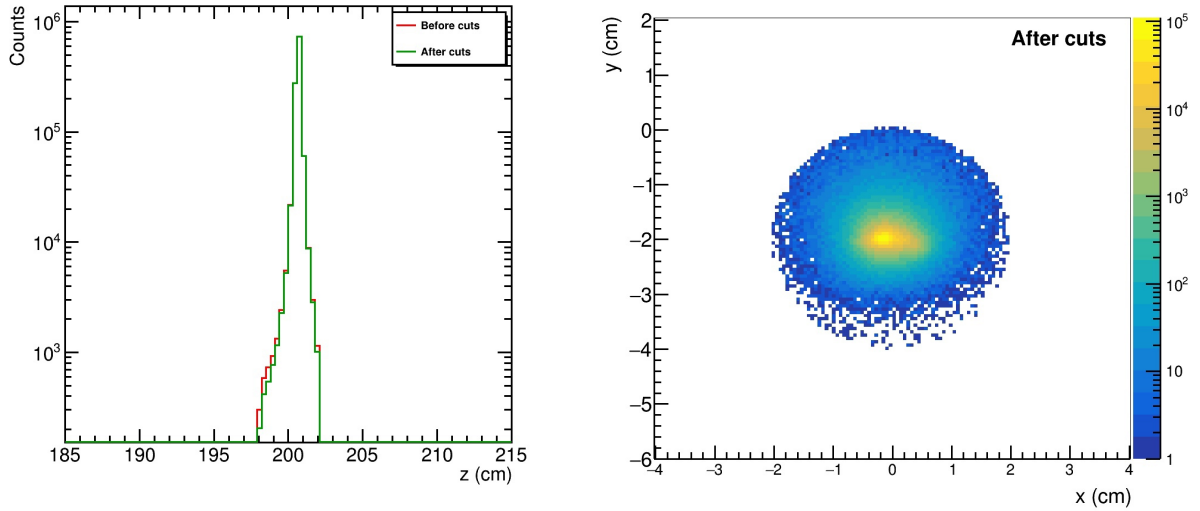


Figure 4: The vertex of the collision of nuclei in the coordinates Z (a), X and Y (b)

To select tracks, some of the distributions presented in the figure 5 were constructed. The red lines show the distributions, where the restrictions on events were taken into account, and the green lines show the distributions for events and tracks. The following restrictions have been chosen:

- $nHits > 15$  - the number of ionization points in the detector, which ensures a fairly accurate reconstruction of the track,
- $0.52 < nHitsFit/nHitsPoss < 4$  - the ratio of the received number of hits (ionization points) in the detector to the total number of hits,
- $0.15 < p < 1.5$  GeV - track momentum (fig. 5 (a)),
- $0.15 < p_T < 1.5$  GeV - transverse momentum of the track ,
- $-2 < \eta < 0$  - pseudorapidity (fig. 5 (b)),
- $0 < DCA < 3$  cm - where DCA - Distance of Closest Approach - the shortest distance from the track to the collision vertex, particles with high values of the DCA are more likely to be produced from secondary interactions and not in the initial collision of nuclei.



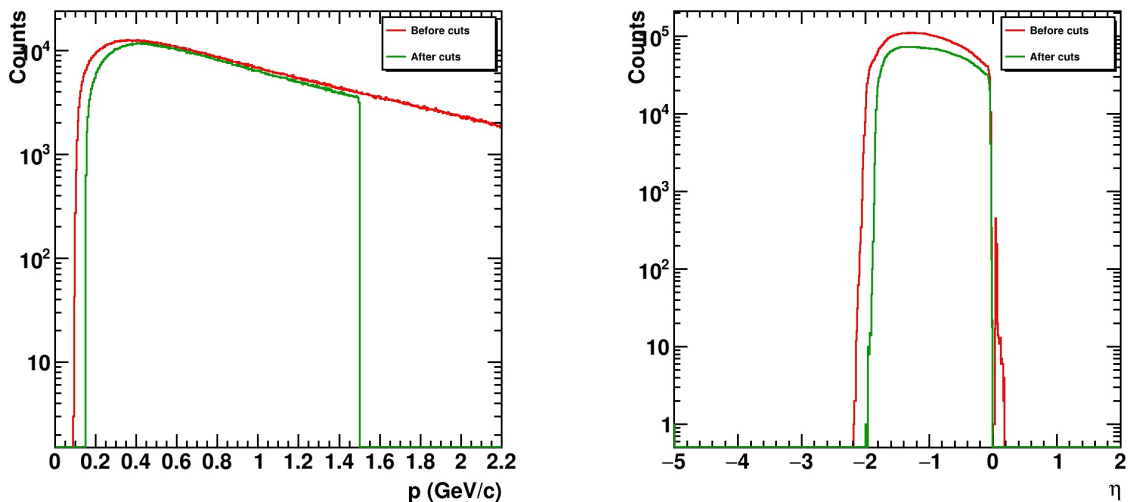


Figure 5: Distribution of track momentum (a) and pseudorapidity (b)

To construct the correlation functions of identical pions, it is necessary to identify the pions in the best possible way. Identification was carried out using the combination of time-projection and time-of-flight systems in the momentum range from 0.15 to 1.5 GeV:

- $0.15 < p < 0.55$  GeV/c:  $|nSigma(Pion)| < 2$ ,  $|nSigma(others)| > 2$ , where  $nSigma$  is deviation of experimentally measured ionization losses from theoretical ones,
- $0.55 < p < 1.5$  GeV/c:  $|nSigma(Pion)| < 3$ ,  $-0.05 < m^2 < 0.08$  GeV<sup>2</sup>/c<sup>4</sup>,  $|1/\beta - 1/\beta(\pi)| < 0.015$ , where  $\beta$  is the particle velocity.

Thus, based on all of the above, charged pions were identified using restrictions on events, tracks, and particles.

To construct the correlation functions of identical pions, it is necessary to select pairs of particles that belong either to the same event or to different events (to suppress quantum-statistical correlations). During the reconstruction of tracks, the effects of merging or splitting tracks may occur. Merging tracks means that one track is reconstructed as a pair of tracks, while splitting means that two tracks are reconstructed as one [7].

In order to correctly split tracks, each track is assigned some binary code, the length of which can be a maximum of 45 (one bit for each pad), where 1 means the presence of a hit in this row of pads, and 0 means its absence. By comparing the resulting set of codes, we can estimate the probability of splitting tracks. The figure 6 shows an example of track reconstruction, where sets of circles and rectangles represent impact from separate tracks. On the left, two separate tracks are shown, and on the right, a candidate for splitting tracks.

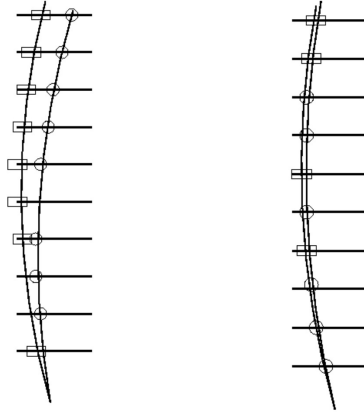


Figure 6: An example of track reconstruction. On the left - separately reconstructed tracks, on the right - a candidate for splitting tracks

To evaluate how track splitting affects correlation functions, the notion of a splitting level (Splitting Level - SL) is introduced:

$$SL = \frac{\sum_{i=1} S_i}{Nhits_1 + Nhits_2}, \quad (7)$$

where  $S_i = +1$  if only one track from a pair has a hit,  $S_i = -1$  if both tracks from a pair have hits,  $S_i = 0$  if none the track has no hit in the detector plane.  $Nhits_1 + Nhits_2$  is the sum of the hits of the two tracks.

Below are plotted dependences of SL on the four-momentum of a pair of particles from one event (fig. 7 (a)) and from different events (fig. 7 (b)).

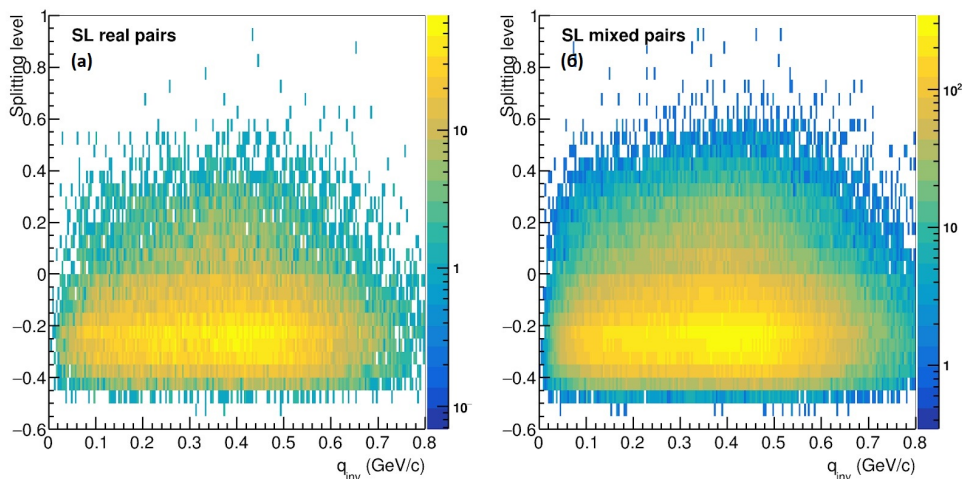


Figure 7: Dependences of the splitting level on the four-momentum pairs of particles from one event - "real pairs" (a) and from different events "mixed pairs" (b)

From the fig. 7 observed that SL mostly varies from -0.5 to 0.6. Based on this distribution, one-dimensional correlation functions of identical pions were constructed depending on various restrictions on SL (figure 8). To construct this distribution, centrality 0-5% and the range of small transverse momentum of pairs were chosen.

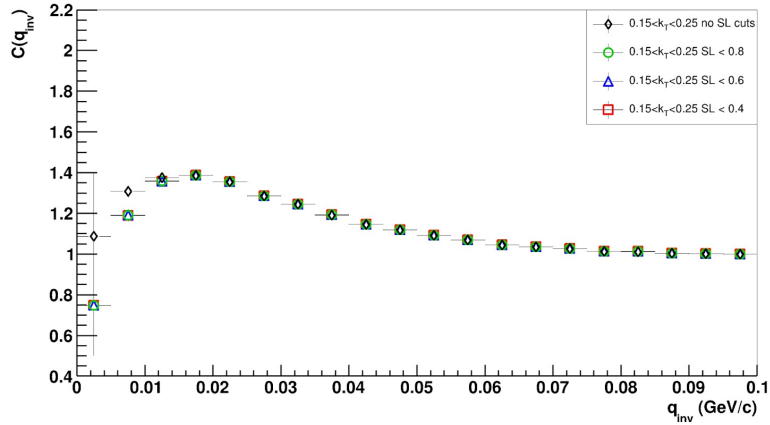


Figure 8: One-dimensional correlation function of identical pions under different constraints on the Splitting Level

It can be seen from the figure above that the correlation function stops changing when the value of SL does not exceed 0.6.

Thus, one of the selected restrictions for further construction of three-dimensional correlation functions will be the selected range per splitting level, which does not exceed 0.6.

On the other hand, the effect of track merging also affects the correlation function of identical pions. The fraction of merged tracks (Fraction of Merged Hits - FMH or Fraction of Merged Rows - FMR) is estimated as the ratio of the number of merged hits to the maximum possible number of hits for track reconstruction - 45. Figure 9 shows the dependence of FMR on the four-momentum of pairs of particles from one event and from different events.

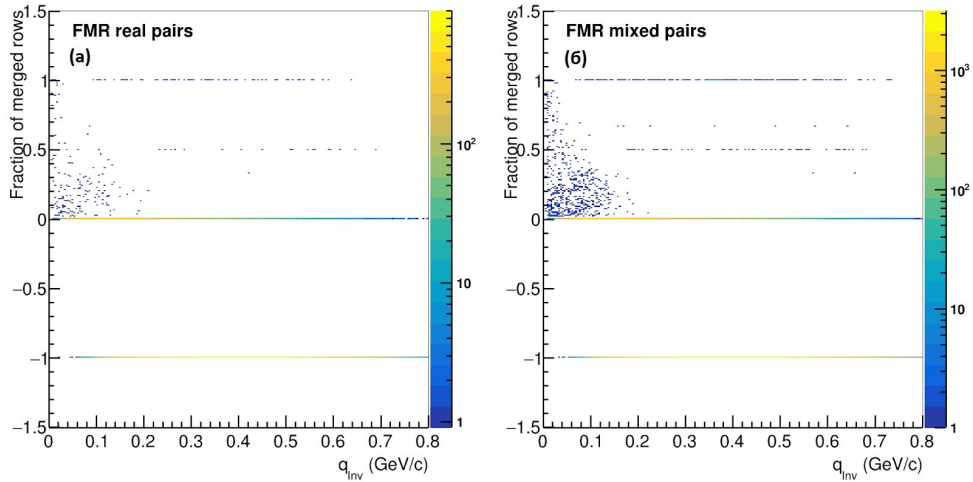


Figure 9: Dependences of the proportion of tracks merging on the four-momentum pairs of particles from one event - "real pairs" (a) and from different events - "mixed pairs" (b)

From the 9 figure, it can be seen that FMR basically has the values 1, which corresponds to the maximum possible proportion of merging tracks, 0 when the merging proportion is minimal, and -1 if the tracks fell into different sectors of the detector.

FMR affects the correlation function of identical pions (fig. 10).

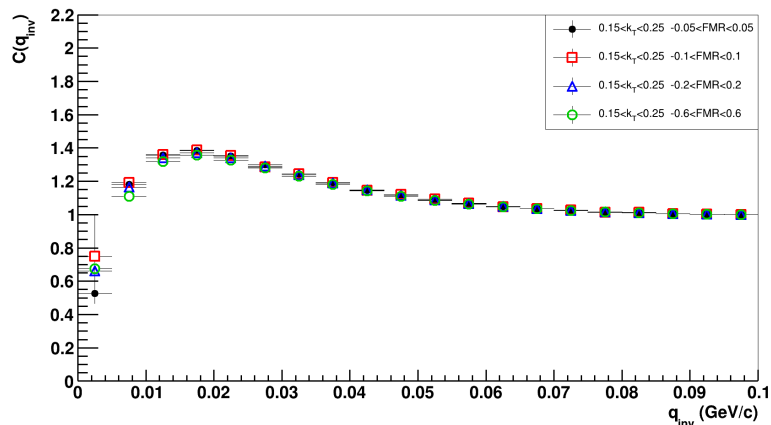


Figure 10: One-dimensional correlation function of identical pions under different constraints on the Fraction of Merged Rows

So, based on the figures above, another limitation on particle pairs is the  $-1.1 < FMR < 0.1$  range, which eliminates the track merging effect.

### 3.1 Results

To construct the correlation functions of identical pions, we used the restrictions on events, tracks, and particles, as well as on pairs of particles, which were described earlier. The distributions were plotted in the centrality ranges 0-10%, 10-40%, 40-80% (an increase in centrality values corresponds to more peripheral collisions) and in the range of transverse momentum of pairs of particles  $0.15 < k_T < 0.55$  GeV, divided into 4 smaller ranges. Correlation functions for positive (red dots) and negative (blue dots) pairs of pions and their fits were built separately, their ratio is also shown (fig. 11). The distributions were fitted using the Bowler-Sinyukov function.

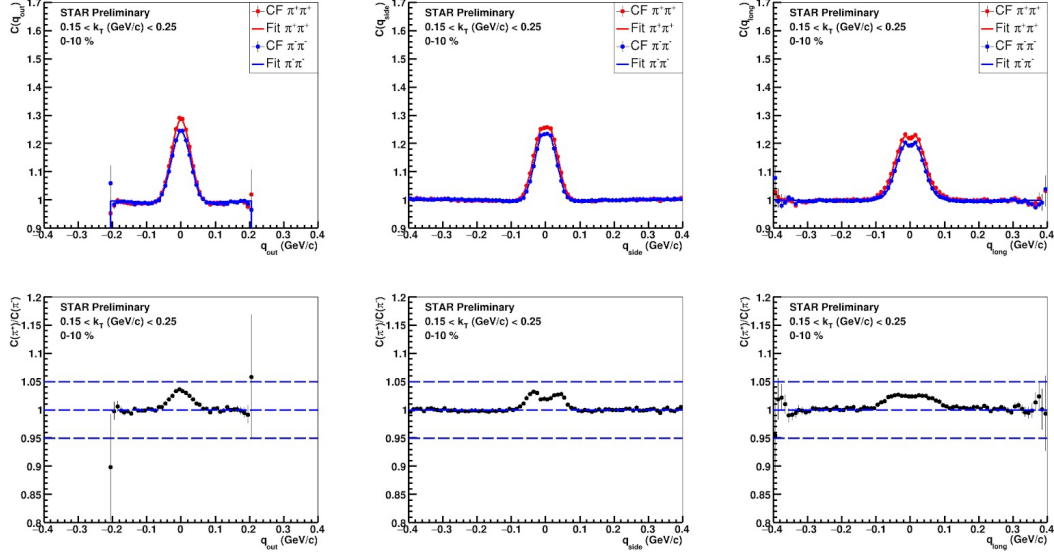


Figure 11: Projections of the correlation function of identical positive (red dots) and negative (blue dots) pions and their fits for collision centralities of gold nuclei 0-10% in the range  $0.15 < k_T < 0.25$ : at the top left - "out", middle - "side", right - "long". The ratio of correlation functions in coordinates is presented at the bottom.

For clarity, the correlation functions were constructed for a fixed range of the transverse momentum of particle pairs depending on different centrality ranges, and vice versa (fig. 12, 13).

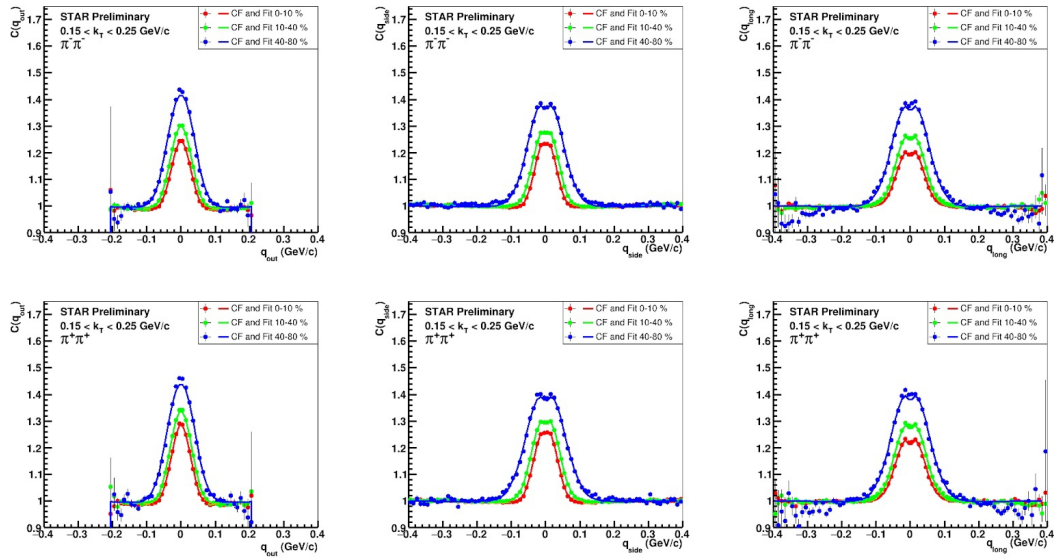


Figure 12: Projections of the correlation function of identical negative and positive pions and their fits for the range  $0.15 < k_T < 0.25$  and for all ranges by centrality: 0-10%, 10-40%, 40-80%

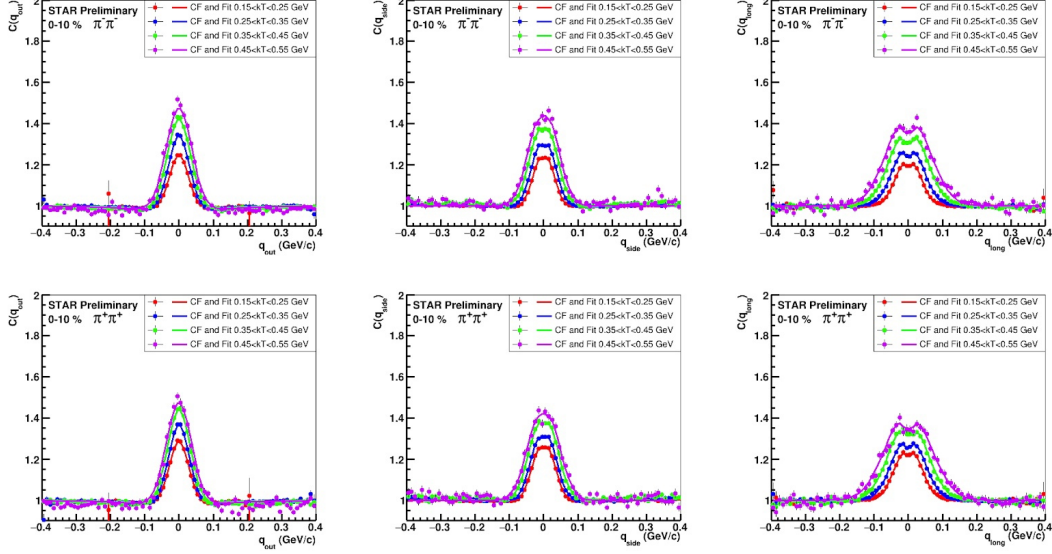


Figure 13: Projections of the correlation function of identical negative and positive pions and their phytes for the centrality range 0-10% and for all ranges of transverse momentum of particle pairs

It can be seen from fig. 12 and 13 that the larger the transverse momentum of pairs of particles or the value of centrality, the smaller the radius of the particle emission region is.

The parameters of the particle emission region (radii of the emission region  $R$ ) extracted by fitting the correlation functions were plotted depending on the ranges in the transverse momentum  $k_T$  (fig. 14). The values of  $k_T$  have been shifted for clarity.

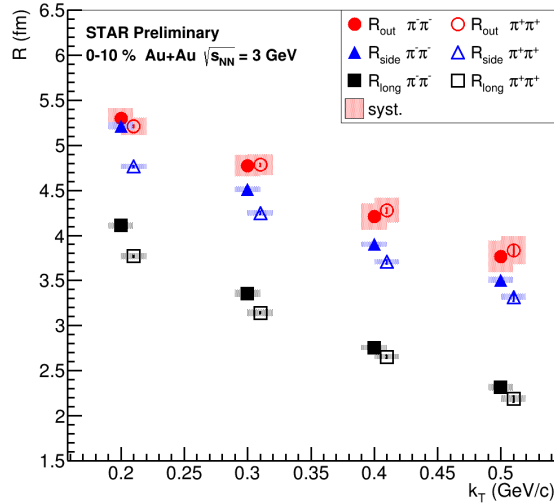


Figure 14: Radii dependence ( $R_{out}$ ,  $R_{side}$ ,  $R_{long}$ ) as a function of the  $k_T$  for the centrality range 0-10% at  $\sqrt{s_{NN}} = 3$  GeV in Au+Au collisions

Femtoscopic radii decrease with increasing  $k_T$  due to a decrease in the emission region of the system due to transverse flow.

## 4 Summary

In this work, quantum-statistical correlations of identical pions produced in collisions of gold nuclei at a center-of-mass system energy of 3 GeV have been studied. A combination of TPC and TOF was used to identify the particles.

Criteria for selecting events, tracks, and particles were developed in this work, with the help of which the identification of charged pions was carried out. The restrictions on pairs of particles necessary to eliminate the effects of merging and splitting of particle tracks are determined. Projections of the three-dimensional correlation function are constructed depending on the relative 4-momentum of a pair of particles for 3 centrality ranges: 0-10%, 10-40%, 40-80%. The resulting projections were fitted with the Bowler-Sinyukov function. As a result, the dependence of the extracted values of the radii of the particle emission region on the transverse momentum of the pairs is obtained, which makes it possible to obtain an idea of the dynamics of the development of the colliding system. Femtoscopic radii decrease with increasing  $k_T$  due to a decrease in the emission region of the system due to transverse flow.

## References

- [1] B. Hanbury *et al.*, Nature **178**, 1046 (1956)
- [2] G. Goldhaber and S. Goldhaber, Phys. Rev. **120**, 300 (1960)
- [3] G. Kopylov and M. Podgoretsky, Sov. J. Nucl. Phys. **15**, 219 (1972)
- [4] G. Kopylov and R. Weiner, Phys. Lett. B. **50**, 472 (1974)
- [5] V. Emelyanov, S. Timoshenko and M. Strihanov, PhysMathLit., 184 (2004)
- [6] F. Yano *et al.*, Phys. Lett. B. **78**, 556 (1978)
- [7] J. Adams *et al.*, Phys. Rev. C. **71**, 044906 (2005)
- [8] M. Lisa *et al.*, Ann. Rev. Nucl. Part. Sci. **55**, 357 (2005)
- [9] J. Adamczewski-Musch *et al.*, Eur. Phys. J. A. **56**, 140 (2020)
- [10] S. Akkelin and Y. Sinyukov, Phys. Lett. B. **356**, 525 (1995)
- [11] K. Ackermann *et al.*, Nucl. Instrum. Meth. A. **499**, 624 (2003)
- [12] J. Adams *et al.*, Phys. Rev. C. **103**, 3 (2021)